

73215

DRAFT

Aphanitic Impact Melt Breccia
1062 grams



Figure 1: Top surface of 73215,9 showing micrometeorite pits and interior, flow-banded matrix.
NASA S90-27756. Cube is 1 inch and scale is marked in cm/mm.

Introduction

Ryder (1993) provided a thorough review of the science that had been accomplished on breccia sample 73215 up to that point. This sample is noteworthy in that it contains a collection of rock clasts with a range of petrologic types and ages (James et al. 1977, Jessberger et al. 1977).

73215 is a polymict breccia that was collected from the rim of a 10 meter crater that was in turn on the rim of Lara Crater (500 m). It is part of the light mantle material from the landslide off of South Massif and is

generally thought to be Serenitatis ejecta (Wolfe et al. 1981). It has micrometeorite craters on one side (figure 1) and an exposure age of ~240 m.y.

Petrography

Lunar sample 73215 is essentially a collection of rock clasts included in an aphanitic, banded matrix of mineral debris. It has been cut into four pieces, two “butt ends” (,8 and ,9) and two parallel slabs (figures 4, 9, 23 and 24). The first slab cut from 73215 was carefully studied by a large consortium of scientists led by Odette James (see James et al. 1975, James 1976,

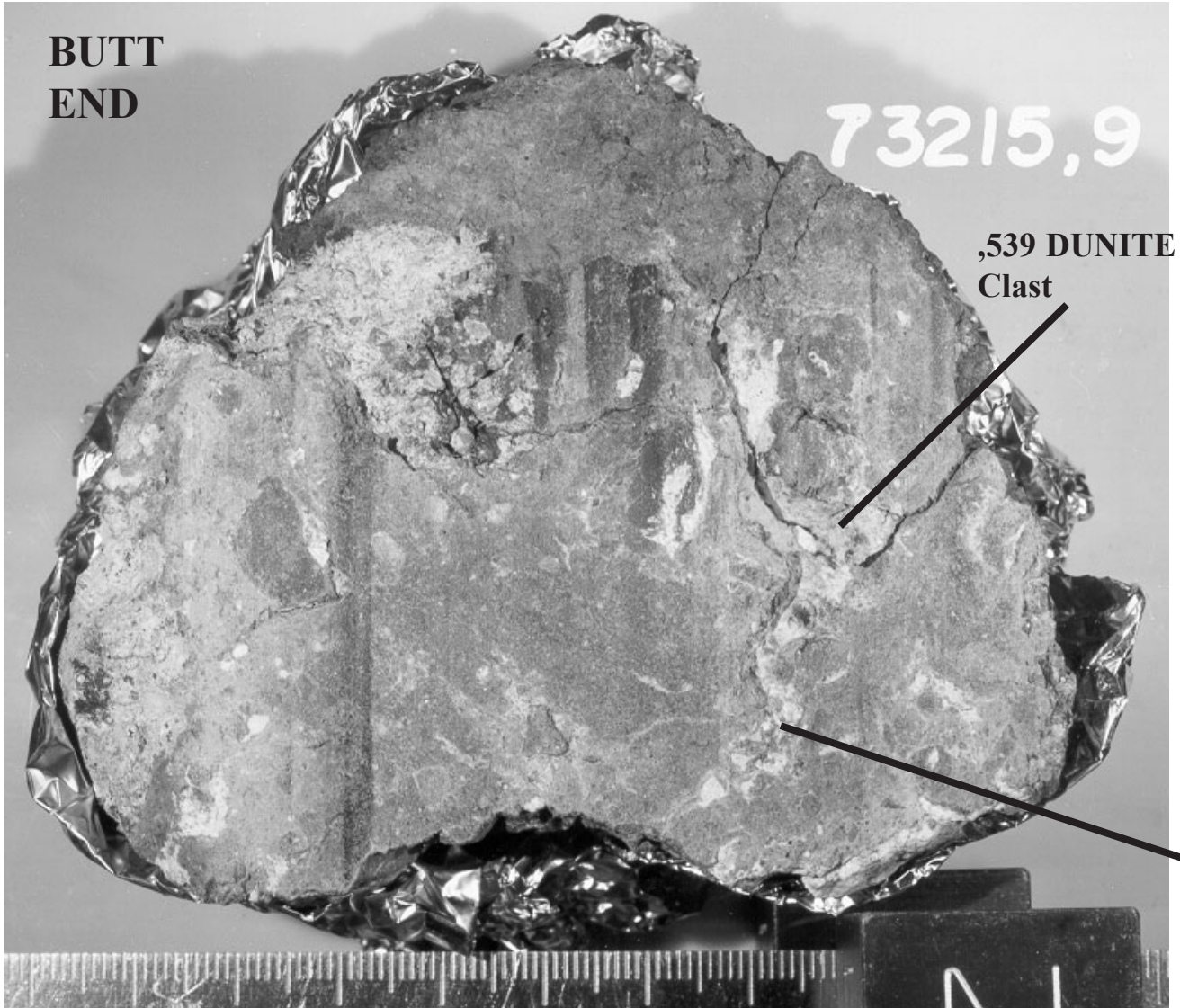


Figure 2: Photo of sawn surface of 73215,9 (butt end) showing light and dark clasts in a banded aphanitic matrix. NASA S90-27755. Cube is 1 inch and scale is in mm/cm.

James and Hammerstrom 1977 and associated papers). The second slab revealed additional clasts, some of which were studied by Eckert et al. (1994a, b) and Neal and Taylor (1998).

The matrix of 73215 is described in detail by James and 18 others (1975). Chemical analyses of various portions of the matrix proved to be generally similar (table 1 a, b)(Blanchard et al. 1976). The overall structure of 73215 (figures 2, 23) is dominated by “flow banding” formed by differential flow and /or shear during and after aggregation and consolidation. Minute white lines that are traces of planes of fine-scale shear are visible in all types of matrix and schlieren derived from flattened clasts are oriented parallel to shear planes. Abundant small lithic and mineral fragments

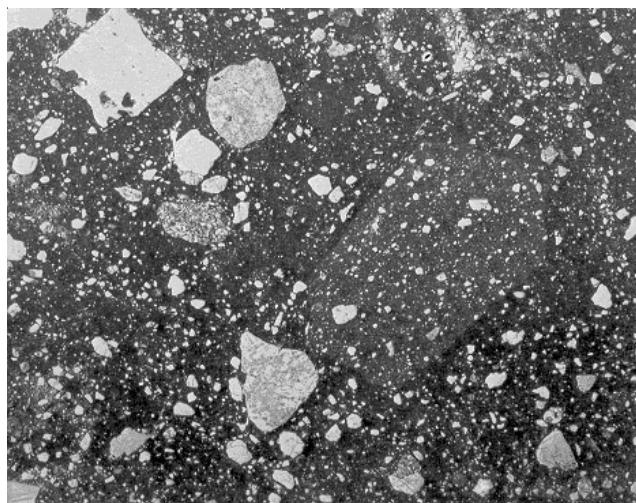


Figure 3: Photomicrograph of thin section of 73215 showing clastic nature of matrix (from James 1976). Field of view is 13 mm.

SECOND SLAB

,526

WI

,534
*Spinel
Troct-
olite
Clast*

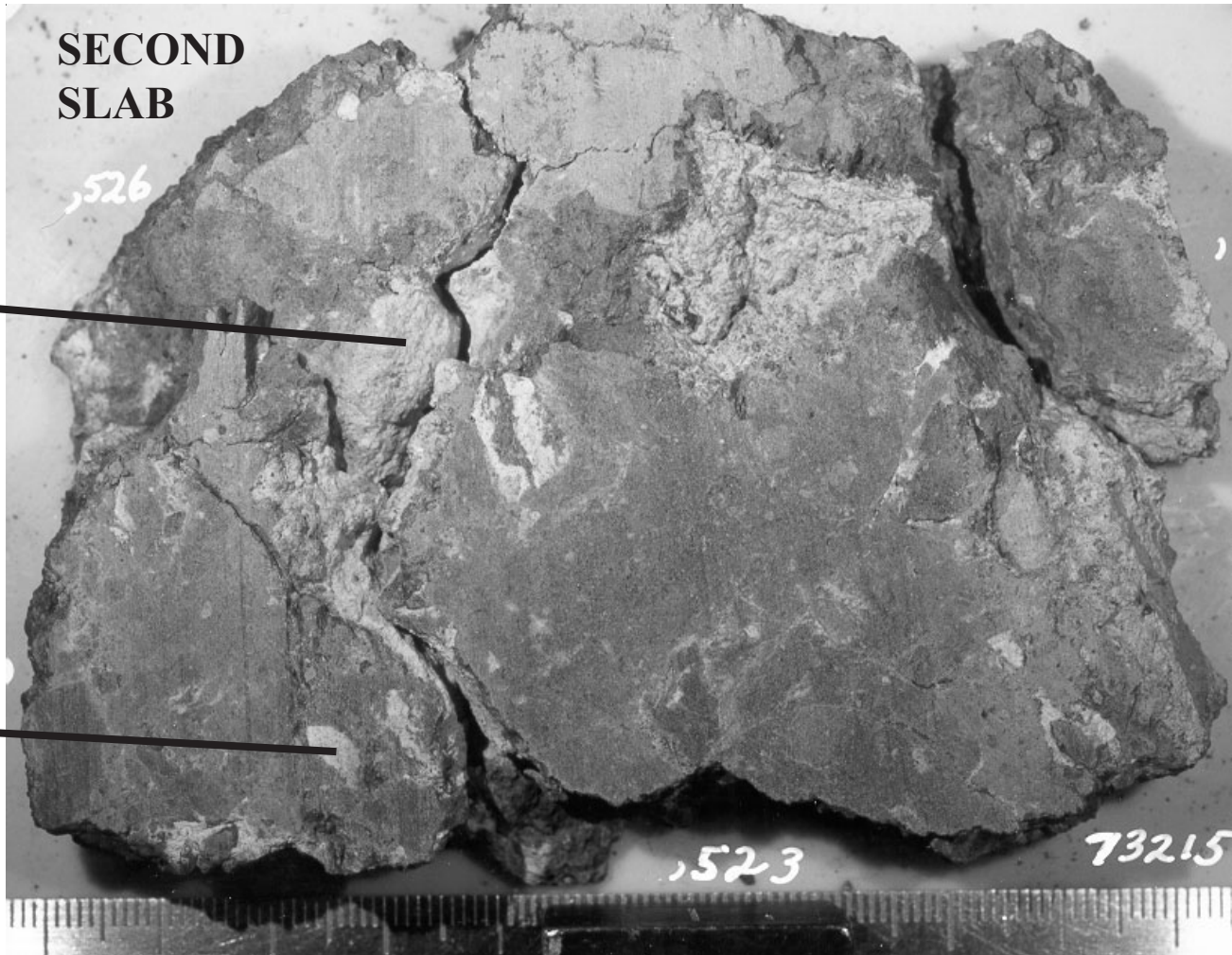


Figure 4: Photo of second slab cut from 73215 in 1988 showing prominent clasts in banded, aphanitic matrix. NASA S88-46201. This sawn surface matches that of the butt end (figure 2). Scale is in mm/cm.

are set in a dark aphanitic groundmass with minute grain size (figure 3). The grain size distribution appears seriate (figure 5). Reflected light shows that the matrix has a fine wormy porosity. An analysis of the modal mineralogy of grains >5 microns shows general similarity of the different matrix types and with the aphanitic clast (James 1976).

Dence et al. (1976) and Dence and Grieve (1976) described 73215 as genetically comparable with terrestrial suevites although, for some reason, there is not much evidence for shock and/or thermal history.

Important Clasts

Felsite 43,3

Perhaps the most important clast in 73215 is the small (~20 mg) felsite clast (43-3) that was studied by the James Consortium, because the rather precise crystallization age obtained for this small clast has been used to establish the age of this breccia, which is then interpreted as the age of the Serenitatis Impact (Wolfe et al. 1981). Warren (1993) lists it as possibly pristine.

Mineralogical Mode of Matrix (73215) (from James 1976)

	Groundmass	mafic minerals	plagioclase	lithic
Gray aphanitic	68	8.2	23.7	
Black aphanitic	71.1	5.1	20.5	3.3
Schlieren-rich gray	65.7	10.9	23.4	
Gray spheroid clast	60.8	13.8	22.2	3.2
Black aphanitic clast	68.8	7.9	23.4	0.1

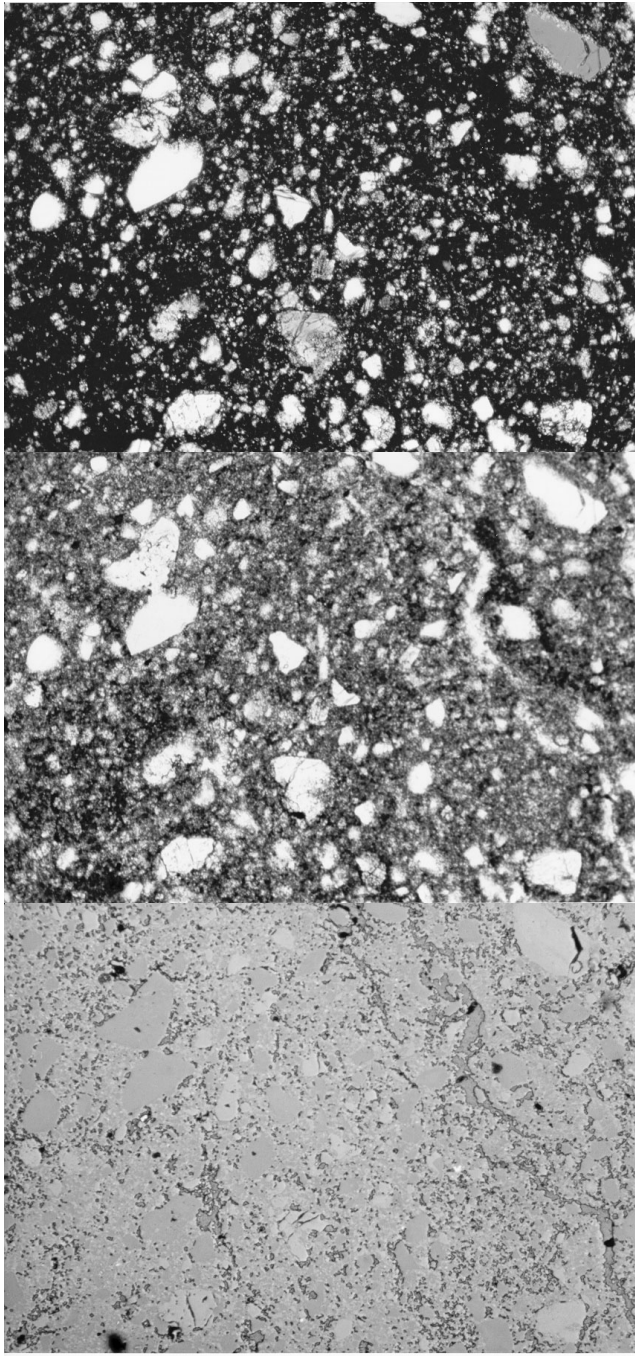


Figure 5: Photomicrographs of thin section 73215,47 showing texture of aphanitic matrix. NASA S79-27761-27763. Polarized, plain and reflected light of same area. Field of view is 1.2 mm.

James and Hammarstrom (1976) describe this clast as partially crystalline and partially glassy. The texture of the crystalline portion is a vermicular intergrowth of quartz (40%) and K,Ba-feldspar (60%). Sparse grains of irregular anhedral plagioclase, blocky ilmenite and ovoid olivine grains are also present. Pyroxene and olivine are Fe-rich (figure 11). Felsic glass

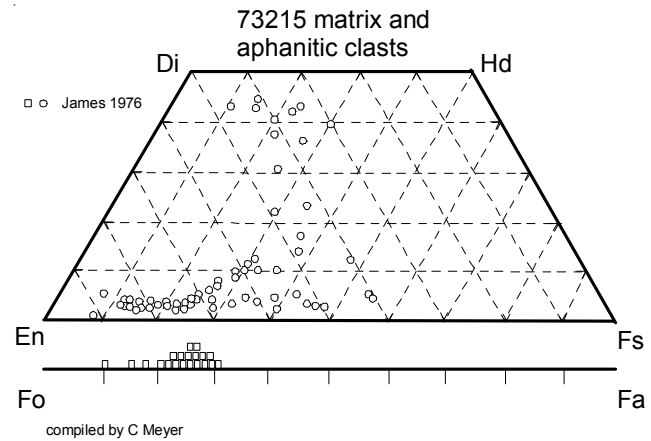


Figure 6: Composition of pyroxene and olivine in fine-grained matrix and aphanitic clasts in 73215 (from James 1976).

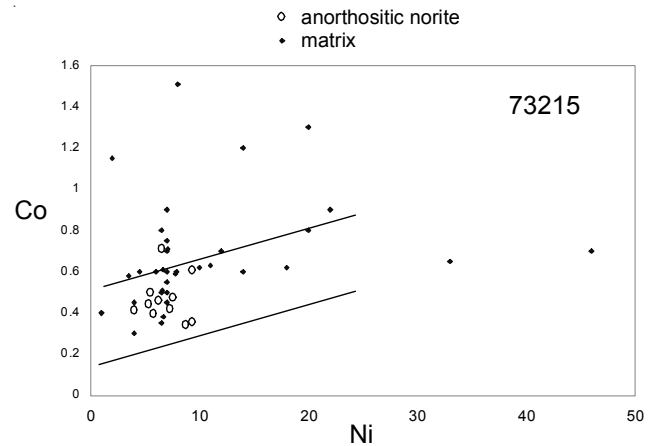


Figure 7: Composition of metal grains in matrix of 73215 (James 1976) and in Anorthositic Norite Clasts (James and Hammarstrom 1977).

surrounds and intrudes the crystalline portion. A variety of minerals, including zircon, are included as relics in the glass (see James and Hammarstrom for a full description). Blanchard et al. (1977) give an analysis (figure 16). Compston et al. (1977) obtained a crystallization age of 3.90 ± 0.05 b.y. by internal Rb-Sr isochron technique (figure 15), confirmed by Jessberger et al. (1977) as 3.92 ± 0.04 b.y. by the Ar-Ar plateau technique (figure 14).

Dunite ,539 ,580 ,7002

The third saw cut, which produced the second slab, exposed a large powdery greenish-tan clast (.539) which proved hard to extract (figures 2, 4). A grain mount showed that it was mostly olivine ($\text{Fo}_{89.93}$) with significant pyroxene (figure 22) and plagioclase ($\text{An}_{91.96}$) as well as trace spinel (Eckert et al. 1991 and Neal and Taylor 1998). The analysis of ,539 showed low

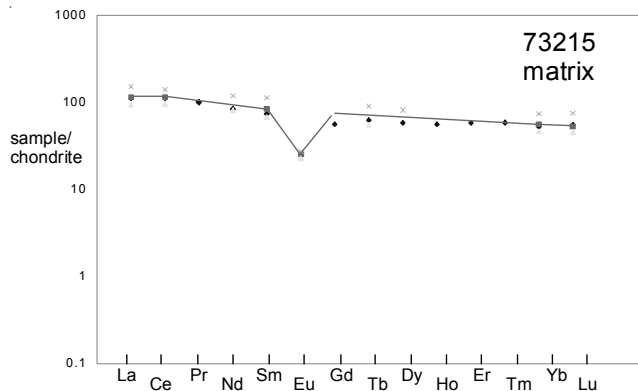


Figure 8: Bulk composition of matrix units in 73215 (from Bence and Taylor 1975, James et al. 1975 and Blanchard et al. 1976).

Eu (figure 18), but significant REE (possibly contamination). This dunite clast appears to deserve more attention.

Spinel Troctolite ,534 ,579 ,7001

Spinel troctolite ,534 (figure 4) has a recrystallized porphyroblastic texture with about 20% olivine (Fo_{89-92}), 78% plagioclase (An_{91-96}) and ~2% Al-spinel ($Cr+Al=10$) and minor amounts of pyroxene (figure 21), Fe-Ni metal and chromite (Eckert et al. 1991, Neal and Taylor 1998). It has a positive Eu anomaly (figure 18).

Spinel Troctolite ,32

Bence et al. (1975) were the first to recognize spinel troctolite as a clast type in 73215 (table 2a, figure 16).

Spinel Troctolite-basalt ,170

A 5 mm clast ,170 has been described as a pink-spinel-bearing troctolitic basalt by James and Hedenquist (1978). Texturally the clast consists of patches of basaltic-textured rock enclosed by very fine grained granoblastic rock. The calculated mode is ~52% olivine (Fo_{82-87}), 5% low-Ca pyroxene (Wo_4En_{84}), 6% high-Ca pyroxene ($Wo_{44}En_{50}$), 36% plagioclase (An_{84-95}), trace chromite and ilmenite. Blanchard et al. (1977) and Higuchi and Morgan (1975) produced analyses (table 2). Jessberger (1979) determined a high temperature Ar-Ar release age of 4.46 ± 0.04 b.y. (figure 20).

Anorthositic Norite 29,9 coarse-grained

This prominent clast (figures 9, 25) has granulitic, relatively coarse-grained texture with blocky subhedral plagioclase grains (An_{95}) (up to 1 mm), rounded irregular olivine grains (Fo_{70-75}) (0.2 mm) and minor augite “globules” ($Wo_{40}En_{45}$) poikilitically enclosed in orthopyroxene (Wo_4En_{75}) (1 mm) (James and Hammarstrom 1977). It has been analyzed by

Blanchard et al. (1977) and Morgan et al. (1979) (table 2a, figure 18).

Anorthositic Norite 46,25 46,33

James and Hammarstrom (1977) termed this clast “anorthositic gabbro”, but it is compositionally a norite or texturally a “granulite”. Equant plagioclase (An_{95}) and olivine (Fo_{78}) crystals form a mosaic with grain junctions commonly at 120 degree angles. Pyroxene forms oikocrysts scattered throughout the matrix (figure 17). Blanchard et al. (1977) give analyses (figure 18) and Compston et al. (1977) found it fit a 4.24 b.y. isochron (figure 19).

Aphanitic Clasts “BC” and “GS”

James (1976) and Blanchard et al. (1976) described the dark fine-grained aphanitic clasts in 73215 showing that they were made of the same materials as the matrix of 73215 (only more densely packed and finer grained).

Large Clast

The obvious large triangular clast (1 inch) exposed by the third saw cut (figures 2 and 4) appears to not have been studied (probably because it is itself a breccia).

Chemistry

The bulk chemical composition of 73215 and related aphanitic matrix samples of the South Massif is generally similar to that of the micropoikilitic boulder samples from the North Massif (Wolfe 1981). Eldridge et al. (1974) reported U, Th and K determined by radiation counting of the whole rock (table 1b). These values are similar to that determined on much smaller samples of the matrix by various investigators (table 1). Bence et al. (1975) were the first to report analyses of matrix and clasts in 73215 (tables 1 and 2, figure 8). These results were confirmed by the analyses of Blanchard et al. (1976, 1977).

A wide variety of lithic clasts have been recognized – from felsite to dunite (table 2). The composition of the dunite (,539) and spinel troctolite (,534) clasts in 73215 was determined by Roman Schmitt and reported by Neal and Taylor 1998 (table 2b, figure 18). Although these clasts are probably pristine, they could not be extracted cleanly from the breccia matrix and show some Ir and Au content.

Radiogenic age dating

Jessberger et al. (1977) reported Ar-Ar plateau ages for a large number of sub-samples of 73215 – matrix and clasts (table 3). They noted that some clasts had a high-temperature plateau that was older than a low-temperature plateau and reported two ages for these

Table 1a. Chemical composition of 73215 (matrix).

reference	Hertogen77	Ehmann75	black	gray	grey	grey	black	black	schlieren	light	Blanchard76 range	ave. matrix	
			,161	,74	,76	,170	,184	,161	,177	,186			
SiO ₂ %	48.8	(b)	48.1	46.1			46.8	46.1	46.7	(c) 44.9 - 47.6	46.4	(b)	
TiO ₂			0.8	1.1			0.4	1.1	0.6	(c) 0.2 - 1.1	0.7	(b)	
Al ₂ O ₃	21.3	(b)	19.4	21.7			21.5	19.9	20.4	(c) 19.3 - 21.7	20.6	(b)	
FeO	8.5	(b)	7.64	7.39			7.2	7.28		(b) 6.63 - 7.8	7.3	(b)	
MnO	0.1	(b)	0.123	0.104			0.099	0.119		(b) 0.099 - 0.119	0.104	(b)	
MgO	18.1	(b)	10.2	10.2			11.8	11.1	11	(c) 10.2 - 14.8	11.6	(b)	
CaO			11	12.2			11.8	12.3	11.5	(c) 10.5 - 12.3	11.9	(b)	
Na ₂ O		0.51	(b)	0.624	0.495		0.488	0.487		(b) 0.46 - 0.55	0.5	(b)	
K ₂ O				0.656	0.167		0.17	0.191	0.31	(c) 0.17 - 0.31	0.2	(b)	
P ₂ O ₅													
S %													
<i>sum</i>													
Sc ppm			12 - - 17	14.3	14.4		13.5	14.1	23.7	12 - 23.7	14.7	(b)	
V													
Cr			1310 - 1710	1150	1368		1574	1512	3150	(b) 1300 - 3150	1710	(b)	
Co			25 - - 34	24.5	25.6		27.8	21.2	27.1	21.2 - 28.2	25.3	(b)	
Ni	137	(a)		200	150	163	118	190	152	150	110 - 200	165	(b)
Cu													
Zn	1.92	(a)	<5			2	1.9	2.5	2.5				
Ga			4.16						5.3	5.3			
Ge ppb	216	(a)				175	82	252					
As													
Se	111	(a)				72	39	72					
Rb	3.25	(a)		5.5		2.3	2.34	8.9	3	13.6			
Sr													
Y													
Zr			370 - 874										
Nb													
Mo													
Ru													
Rh													
Pd ppb	5.9	(a)											
Ag ppb	0.73	(a)				0.91	20	0.73					
Cd ppb	7.4	(a)				18.4	1.3	12.4					
In ppb	1.77	(a)											
Sn ppb													
Sb ppb	0.84	(a)				0.95	0.89	1.2					
Te ppb	<3.4	(a)				5.9		4.9					
Cs ppm	0.141	(a)		0.18		0.16	0.11	0.56	0.123	0.57			
Ba													
La			41	25.5			25.6	24.3	36.1	22.3 - 36.1	27	(b)	
Ce			105	69			68	63	86	58 - 86	70	(b)	
Pr													
Nd			62					37.3	55				
Sm			18.6	11.9			12.2	10.7	16.8	10.0 - 16.8	12.5	(b)	
Eu			1.63	1.41			1.37	1.35	1.55	1.3 - - 1.63	1.43	(b)	
Gd			20.6					13	15				
Tb			3.55	2.8			2.7	2.11	3.3	2.0 - 3.3	2.6	(b)	
Dy			23.5					14.6	20				
Ho													
Er													
Tm													
Yb			13	8.8			9.1	8.5	12.1	7.6 - 12.1	9.1	(b)	
Lu			1.91	1.2			1.35	1.1	1.84	1.10 - 1.84	1.3	(b)	
Hf		8.6 - 19.7	13.7	9.5			8.9	7.8	13.9	7.8 - 13.9	9.5	(b)	
Ta			2.3	1.5			1.4	1.4		1.0 - 1.8	1.4	(b)	
W ppb								0.34					
Re ppb	0.322	(a)				0.37	0.27						
Os ppb	3.13	(a)											
Ir ppb	3.51	(a)				4.9	3.5	4.3					
Pt ppb													
Au ppb	1.96	(a)				2.7	1.6	2.4					
Th ppm				7.5	3.7			4.2	3.6				
U ppm	1.13	(a)				1.2	1.1	2.2		3.4 - 4.8	4.1	(b)	

technique: (a) RNAA, (b) INAA, (c) AA

Table 1b. Chemical composition of 73215 (matrix cont.).

reference	Eldridge74	Bence75			Higuchi and Morgan75, Morgan76		
weight	,94	,49	,140	,32	,90	,76	,161 ,170
SiO ₂ %	47.67	46.47	46.53	46.75	46.34	(b)	
TiO ₂	0.23	0.63	0.65	0.67	0.68	(b)	
Al ₂ O ₃	23.4	22.95	20.66	20.64	20.07	(b)	
FeO	5.39	6.58	7.73	7.56	7.79	(b)	
MnO							
MgO	9.16	9.39	11.47	11.16	11.79	(b)	
CaO	12.81	13.25	12.1	12.2	11.79	(b)	
Na ₂ O	0.83	0.49	0.58	0.42	0.8	(b)	
K ₂ O	0.2	(a) 0.19	0.23	0.2	0.2	0.31	(b)
P ₂ O ₅							
S %							
<i>sum</i>							
Sc ppm		11	16		(c)		
V		39	52		(c)		
Cr		810	1400		(c)		
Co		19	24		(c)		
Ni		160	200		(c) 163	152	118
Cu					2	2.5	1.9
Zn							(d)
Ga							
Ge ppb					175	252	82
As							(d)
Se					72	72	39
Rb	1.99	4.73	2.2	1.4	7.7	(c) 2.28	8.93
Sr							2.34
Y	87	58	93	85	127	(c)	
Zr	400	208	300	354	665	(c)	
Nb	25.6	16.8	23.6	23.5	42	(c)	
Mo							
Ru							
Rh							
Pd ppb							
Ag ppb					0.91	0.73	20.4
Cd ppb					18.4	12.4	1.28
In ppb							(d)
Sn ppb							
Sb ppb					0.95	1.19	0.819
Te ppb					5.9	4.9	4.7
Cs ppm					0.161	0.55	0.094
Ba	300	211	315	350	432	(c)	
La	26	16.6	25	24.5	37.2	(c)	
Ce	68	41	71	68	99.6	(c)	
Pr	9	5.9	9.8	8.96	13.3	(c)	
Nd	38	22.2	39.9	36.3	53	(c)	
Sm	11	6.42	11.1	9.55	15.6	(c)	
Eu	1.39	1.25	1.45	1.19	1.59	(c)	
Gd	11	8.14	13.9	10.7	18.3	(c)	
Tb	2.28	1.45	2.35	1.98	3.24	(c)	
Dy	14.2	8.8	14.5	12.9	21.3	(c)	
Ho	3.12	2.12	3.3	2.9	4.61	(c)	
Er	9.3	6.2	9.8	8.6	13.9	(c)	
Tm	1.43	0.91	1.44	1.24	2.05	(c)	
Yb	8.67	5.34	8.73	7.51	12.4	(c)	
Lu	1.34	0.86	1.35	1.16	1.93	(c)	
Hf	9.9	6.1	8.41	8	14.5	(c)	
Ta							
W ppb							
Re ppb					0.369	0.336	0.274
Os ppb							(d)
Ir ppb					4.88	4.31	3.49
Pt ppb							(d)
Au ppb					2.71	2.45	1.65
Th ppm	4.05	(a) 4.81	3.49	4.51	4.2	7.3 (c)	
U ppm	1.1	(a) 1.23	0.87	1.24	1.08	1.76 (c) 1.2	2.22
technique: (a) radiation counting, (b) emp, (c) SSMS, (d) RNAA							

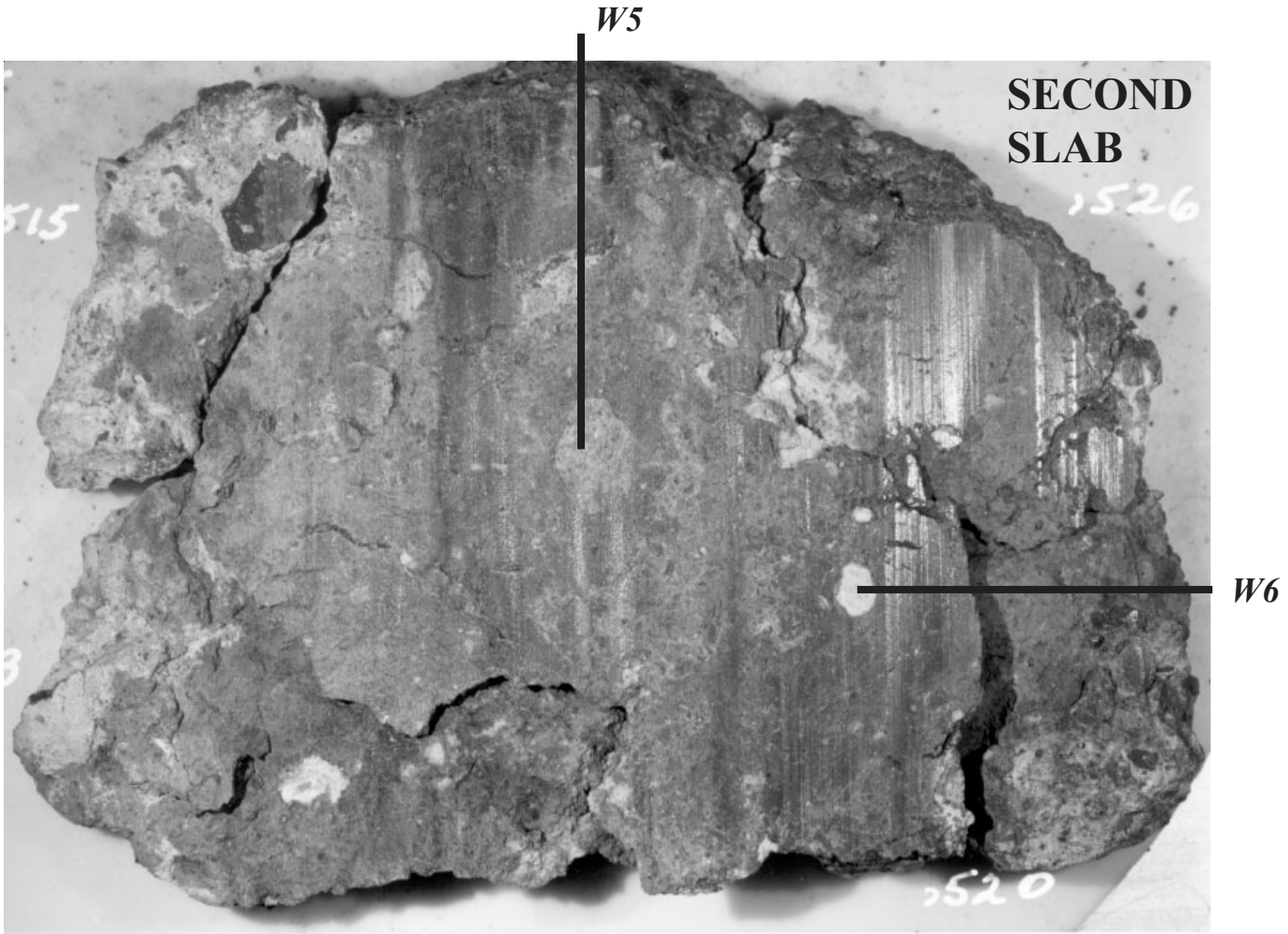


Figure 9: Second slab cut from 73215 showing clasts. Slab broke into pieces (note the cracks). This is the sawn surface opposite the first slab (figure 23). W5 is the same clast as ,29-9. Sample is about 11 cm across.

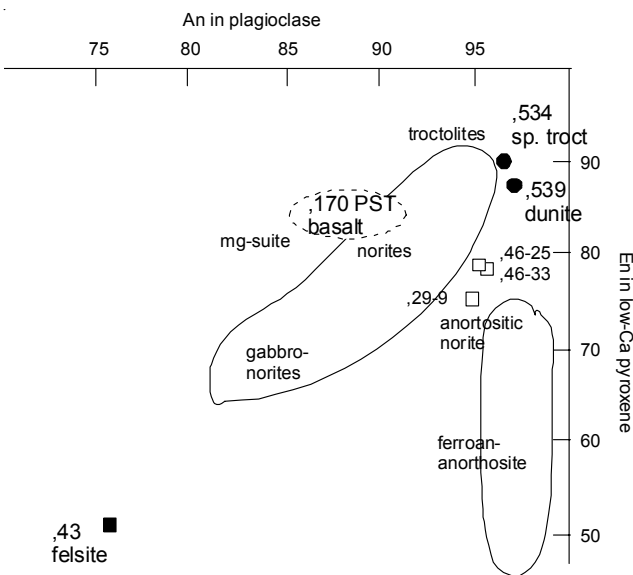


Figure 10: Composition of co-existing mafic minerals and plagioclase in clasts in 73215 (from Neal and Taylor 1998, James and Hedenquist 1978, James and Hammarstrom 1978).

clasts. Muller et al. (1977) and Eichorn et al. (1978) used a pulsed laser to degass Ar from local areas in the interior of clasts and at the margins showing that the clasts were partially degassed during breccia formation. The older ages for the anorthositic norite clasts were generally concordant with the Rb-Sr results of Compston et al. (1977)(figure 19). Jessberger (1979) also obtained an old age (4.42 b.y.) for pink-spinel-bearing troctolitic basalt clast (figure 20).

The concordant age obtained by Ar-Ar and Rb-Sr for the felsite clast (3.92 b.y., old constants) has been used to date the age of the breccia forming event (which, in turn, yields the age the Serenitatis Basin)(Compston et al. 1977, Jessberger et al. 1977, James et al. 1977, Wolfe et al. 1981).

The James Consortium also reported U, Th, Pb and Nd, Sm isotopic data for the matrix of 73215 (James and 18 others 1975).

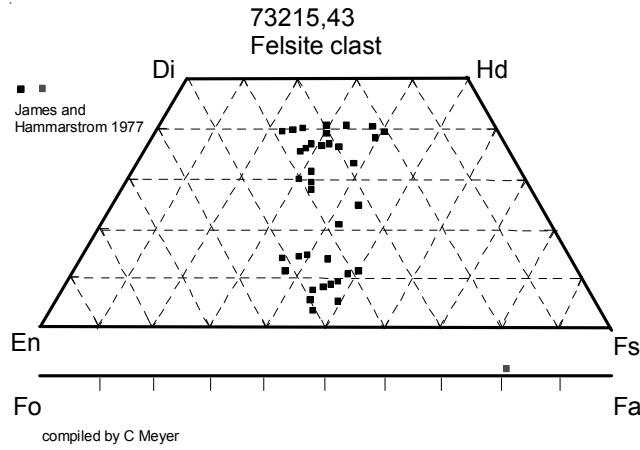


Figure 11: Composition of pyroxene and olivine in felsite clast from 73215,43 (from James and Hammarstrom 1977).

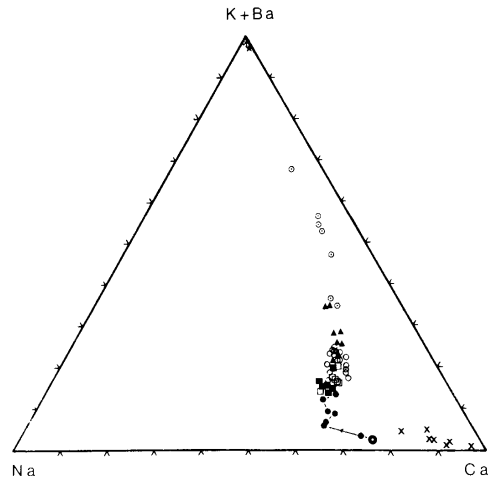


Figure 12: Composition of ternary feldspar in 73215 felsite (James and Hammarstrom 1977).

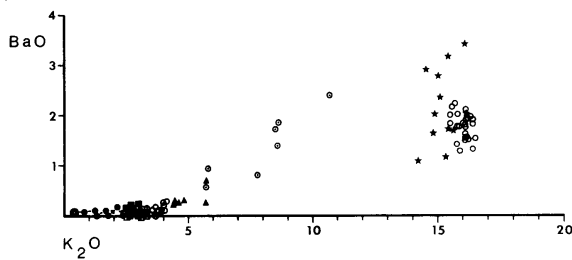


Figure 13: Composition of K,Ba feldspar in 73215 felsite (James and Hammarstrom 1977)

Cosmogenic isotopes and exposure ages

O'Kelley et al. (1974) determined the cosmic-ray-induced activity of ^{26}Al (85 dpm/kg), ^{22}Na (59 dpm/kg), ^{54}Mn (36 dpm/kg), ^{56}Co (51 dpm/kg) and ^{46}Sc (3 dpm/kg). This activity (corrected back to liftoff) was higher than for rocks from earlier missions due to the effects of an intense solar flare in August 1972.

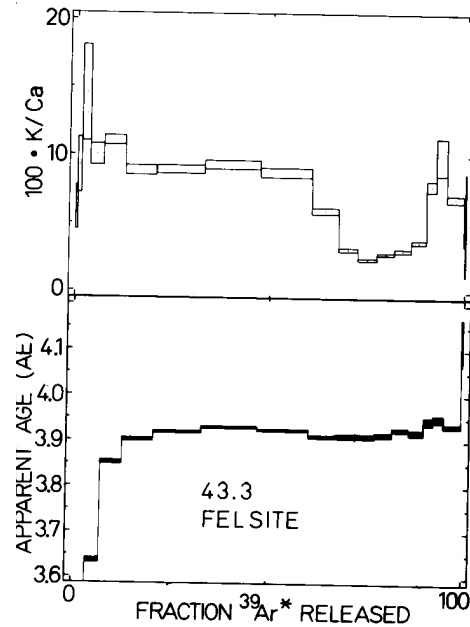


Figure 14: Argon release pattern for felsite clast in 73215 (Jessberger et al. 1977).

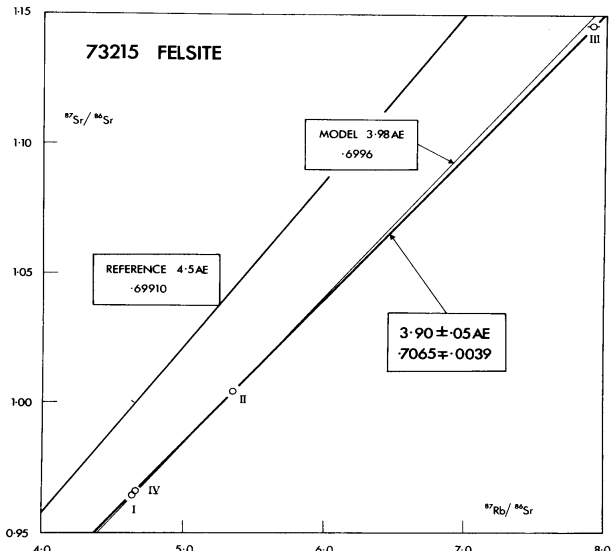


Figure 15: Rb-Sr mineral isochron for felsite clast in 73215 (Compston et al. 1977). Old Rb decay constant.

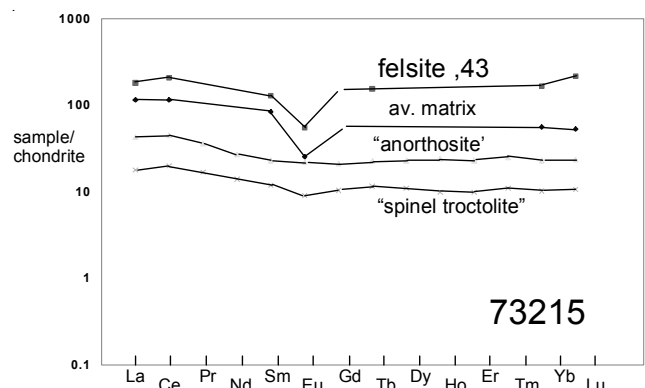


Figure 16: Composition of clasts and matrix in 73215 (Bence et al. 1975, Blanchard et al. 1976).

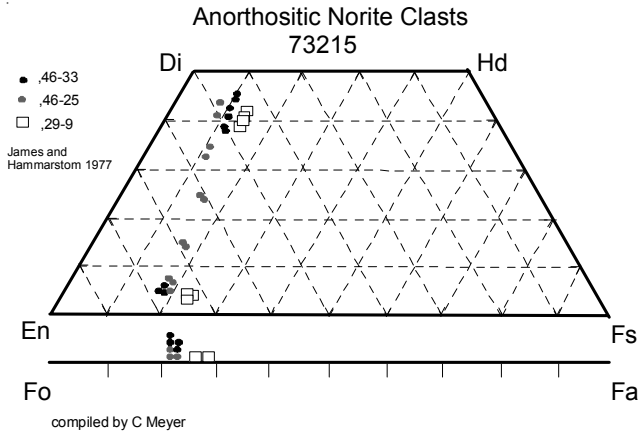


Figure 17: Olivine and pyroxene composition of small "anorthositic norite" clasts in 73215 (James and Hammarstrom 1977).

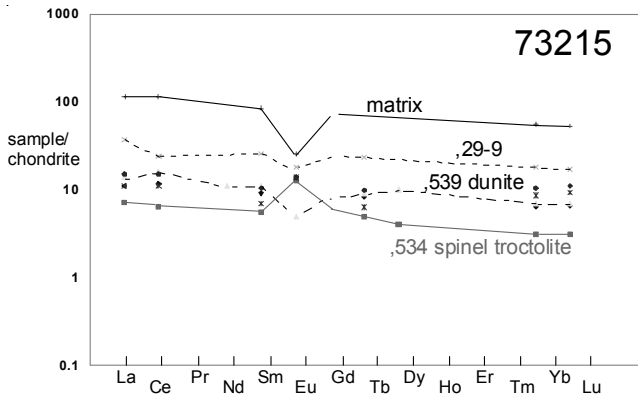


Figure 18: Composition of "anorthositic norite" clasts in 73215 (from Blanchard et al. 1977) and including "spinel troctolite" and "dunite" from Neal and Taylor 1998.

Jessberger et al. (1976, 1977) determined the ^{38}Ar exposure ages (average 244 ± 9 m.y.) in close agreement with the Kr-Kr exposure age 243 ± 7 m.y. determined by Kurt Marti (James and 18 others 1975). This is generally taken as the age of the landslide off of South Massif.

Other Studies

- | | |
|------------------------|------------------------------|
| Housley et al. (1976) | magnetics |
| Brecher (1976) | |
| Hutcheon et al. (1974) | Cosmic ray and fission tacks |
| Braddy et al. (1975) | |
| Goswami et al. (1976) | |

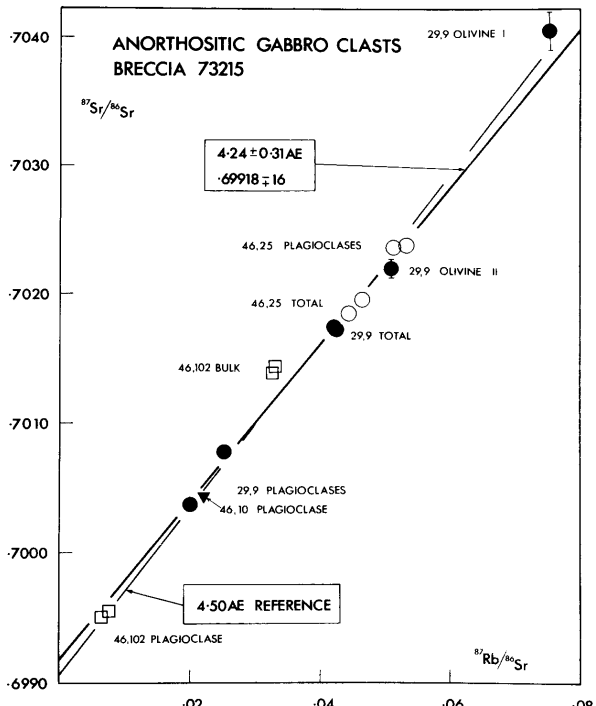


Figure 19: Rb-Sr isochron diagram for several "anorthositic norite" clasts in 73215 (from Compston et al. 1977). Old Rb decay constant.

Processing

Two slabs have been cut from 73215, the **first** in 1973 and the **second**, parallel to the first, in 1988. The first slab was carefully dissected and studied by the James Consortium (James and Blanchard 1976). However, it proved to be difficult to cleanly separate the clasts from the second slab and data for only two of them have been reported. Altogether, 158 thin sections have been prepared for 73215!

Table 3: Summary of argon-argon ages for 73215 (Jessberger et al. 1977). Note that clasts often have two plateau ages! These ages have not been recalculated using new decay constants.

SUBSAMPLE NUMBER	LITHOLOGY	$^{40}\text{Ar} - ^{39}\text{Ar}$ - PLATEAU AGE (AE)				
		3.9	4.0	4.1	4.2	4.3
X 43,3	felsite clast					$3.92 \pm .01$
X 36,2	black		$3.98 \pm .01$			
41,1	black		$4.04 \pm .03$			
X 46,44	light gray	<i>matrix aphanites</i>	$4.02 \pm .01$			
73,1	gray		$4.15 \pm .01$			
177,1	schlieren rich gray		$4.13 \pm .04$			
X 38,32,5	gray spheroid		$4.09 \pm .01$			
38,57,4	gray spheroid	<i>clast aphanites</i>	$4.16 \pm .03$			
X 46,7,3	{vesicular black clast}		$4.02 \pm .01$			
X 46,19,5	{nonvesicular black clast}		$4.08 \pm .01$			
46,10,7	{nonvesicular black clast}		$4.24 \pm .01$			
46,6,1	dark gray clast		$4.17 \pm .07$			
38,39,1,1	troctolite vein		$4.00 \pm .06$			
38,39,1,2	feldspathic clast		$4.11 \pm .05$	$4.28 \pm .03$		
29,9,6	<i>anorthositic gabbro clasts</i>		$4.06 \pm .02$			
46,25,5			$4.24 \pm .01$			
46,33,4			$4.07 \pm .01$	$4.26 \pm .01$		
			$4.07 \pm .01$	$4.22 \pm .01$		

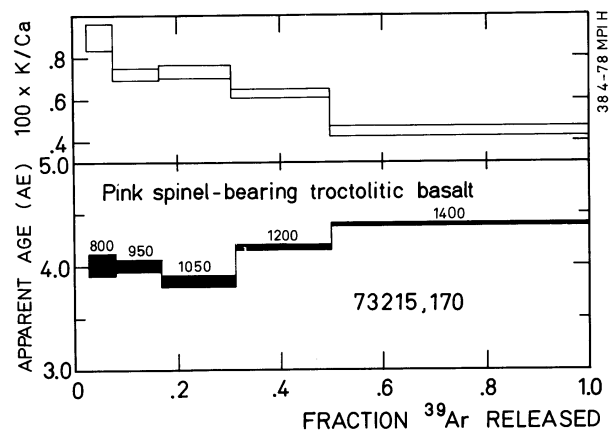


Figure 20: Argon release pattern for pink-spinel troctolitic basalt 73215,170 (from Jessberger 1979).

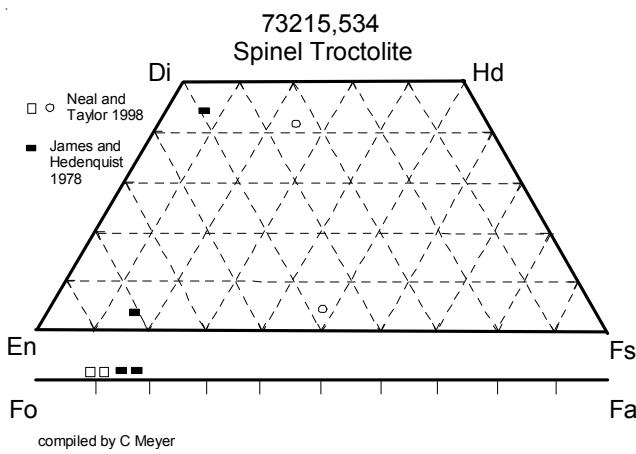


Figure 21: Composition of mafic minerals in PST clasts from 73215 (James and Hedenquist 1978, Neal and Taylor 1998).

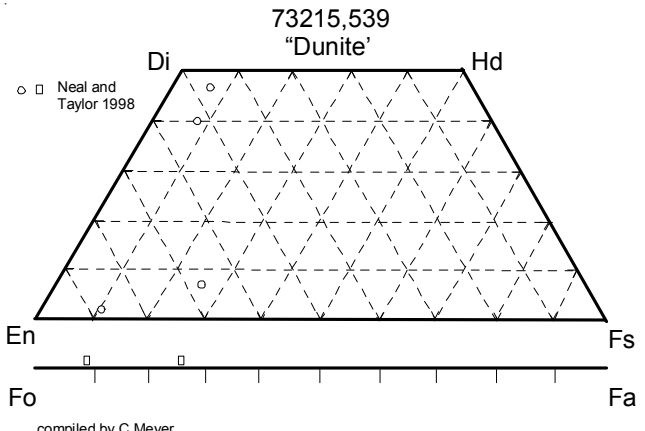


Figure 22: Composition of mafic minerals in clast ,539 from 73215 (Neal and Taylor 1998).

Table 2a. Chemical composition of 73215 (clasts).

	Anor.	Sp.	Troct.	Sp.	Troct.	Anor.	Norite	Morgan79	Anor.	Norite
reference	Bence	75		Blanchard77	Higuchi75	Blanchard77		Compston77	Compston77	
weight	,94	,32		,170-5	,170	,29-9	,29-9	,29-9	,46-25	,46-25 ,46-33
SiO ₂ %	44.47	44.71	(a)	42.8	(e)	45.9	46.6	(e)	44.1	
TiO ₂	0.08		(a)	0.47	(e)	0.69	0.58	(e)	0.23	
Al ₂ O ₃	30.99	31.2	(a)	12.6	(e)	25.6	25.4	(e)	25.6	
FeO	3.03	3.05	(a)	8.6	(e)	4.44	5.14	(e)	5.82	5.1
MnO				0.087	(e)	0.062	0.077	(e)	0.067	
MgO	3.42	3.42	(a)	26	(e)	8.36	8.42	(e)	9.41	
CaO	17.21	17.24	(a)	8.17	(e)	13.9	14.1	(e)	13.8	
Na ₂ O	0.44	0.47	(a)	0.311	(e)	0.43	0.403	(e)	0.356	0.375
K ₂ O	0.1	0.036	(a)	0.06	(e)	0.121	0.097	(e)	0.088	
P ₂ O ₅										
S %										
sum										
Sc ppm				3.7	(d)	7.16	9.04	(d)	7.12	8.2
V										
Cr				1040	(e)	890	1000	(e)	850	840
Co				50.8	(d)	13.7	13.2	(d)	30.7	32.7
Ni				360	(d)	247	(c)	80	(d)	460
Cu										
Zn						6.2	(c)		2	(c)
Ga										
Ge ppb						109	(c)		47	(c)
As										
Se								40	(c)	
Rb	1.88	0.29	(b)			0.297	(c)		2.48	(f)
Sr								167	(f)	2.31
Y	33.7	19.7	(b)							143
Zr	184	79	(b)							
Nb	10.4	6.3	(b)							
Mo										
Ru										
Rh										
Pd ppb								2.1	(c)	
Ag ppb					127	(c)		0.74	(c)	
Cd ppb					3.1	(c)		19.4	(c)	
In ppb								3.2	(c)	
Sn ppb										
Sb ppb						0.706	(c)		66	(c)
Te ppb						2	(c)			
Cs ppm						0.008	(c)			
Ba	182	61	(b)							
La	10.1	4.2	(b)	2.6	(d)	8.7	6.24	(d)	2.61	3.52
Ce	27	12	(b)	7	(d)	24.4	16.8	(d)	6.78	9.1
Pr	3.2	1.54	(b)							
Nd	12.1	6.3	(b)							
Sm	3.4	1.82	(b)	1.34	(d)	3.88	3.08	(d)	1.04	1.53
Eu	1.23	0.5	(b)	0.75	(d)	1	0.91	(d)	0.77	0.77
Gd	4.12	2.05	(b)							
Tb	0.82	0.42	(b)	0.3	(d)	0.84	0.82	(d)	0.23	0.36
Dy	5.6	2.71	(b)							
Ho	1.32	0.57	(b)							
Er	3.67	1.62	(b)							
Tm	0.61	0.27	(b)							
Yb	3.67	1.66	(b)	1.06	(d)	2.9	3	(d)	1.4	1.71
Lu	0.57	0.26	(b)	0.16	(d)	0.413	0.405	(d)	0.225	0.273
Hf	3.15	1.96	(b)	0.9	(d)	3.1	2.2	(d)	1.5	1.4
Ta						0.3	0.2	(d)	0.3	0.16
W ppb										
Re ppb					0.043	(c)		0.167	(c)	
Os ppb								2.3	(c)	
Ir ppb					1.02	(c)		1.78	(c)	
Pt ppb										
Au ppb					2.64	(c)		0.58	(c)	
Th ppm	1.34	0.8	(b)	0.2	(d)	1.6	0.96	(d)	0.53	0.58
U ppm	0.33	0.36	(b)		0.23	(c)		0.36	(c)	

technique: (a) emp, (b) SSMS, (c) RNAA, (d) INAA, (e) AAS, (f) IDMS

Table 2b. Chemical composition of 73215 (clasts cont.).

	Felsite Blanchard77	Sp. Troct. Compston77	Dunite Neal 98	Neal 98
reference				
weight	,43-3	,43	,579	,580
SiO ₂ %			,534	,539
TiO ₂				
Al ₂ O ₃		28.1	6.12	(d)
FeO	2.98	(e)	2.13	8.7
MnO			0.03	0.09
MgO			9.4	40.8
CaO			14.2	3.4
Na ₂ O	0.194	(e)	0.4	0.12
K ₂ O	7	(e)	0.05	0.03
P ₂ O ₅				
S %				
sum				
Sc ppm	4.8	(d)	2.9	3.4
V			28	27
Cr	100	(e)	2080	1010
Co	2.1	(d)	13.1	55
Ni			120	420
Cu				
Zn				
Ga				
Ge ppb				
As				
Se				
Rb		255	(f)	
Sr		158	(f)	180
Y				
Zr				
Nb				
Mo				
Ru				
Rh				
Pd ppb				
Ag ppb				
Cd ppb				
In ppb				
Sn ppb				
Sb ppb				
Te ppb				
Cs ppm				
Ba			28	52
La	42.9	(d)	1.69	3.4
Ce	125	(d)	3.9	9.8
Pr				
Nd			4.9	(d)
Sm	19	(d)	0.83	1.61
Eu	3.11	(d)	0.7	0.28
Gd				
Tb	5.6	(d)	0.19	0.32
Dy			0.98	2.4
Ho				
Er				
Tm				
Yb	27.2	(d)	0.5	1.18
Lu	5.3	(d)	0.075	0.174
Hf	25.6	(d)	0.35	1.39
Ta	5.4	(d)		
W ppb				
Re ppb				
Os ppb				
Ir ppb				
Pt ppb				
Au ppb			4	8
Th ppm	39.9	(d)	0.2	0.62
U ppm				0.17

technique: (a) emp, (b) SSMS, (c) RNAA, (d) INAA, (e) AAS, (f) IDMS

Table 2c. Chemical composition of 73215 (aphanite clasts).

	,46-10	,46-19	,38-57	,38-57	,46-10	,38-57
reference	Blanchard76	Morgan76, Gros76		Morgan79	James 76	
weight					Black Clast	Grey Spheroid
SiO ₂ %	45.6	46.3	45.9	(a)	47.7	46.8
TiO ₂	1.1	1	0.8	(a)	0.96	0.95
Al ₂ O ₃	19.8	20	20.7	(a)	18.1	20
FeO	8.13	7.87	6.94	(a)	7.89	6.86
MnO	0.106	0.111	0.093	(a)	0.09	0.07
MgO	12	11.7	11.8	(a)	12.4	11.8
CaO	11.5	11.7	11.4	(a)	11.6	12.2
Na ₂ O	0.52	0.54	0.52	(a)	0.57	0.61
K ₂ O	0.22	0.22	0.16	(a)	0.24	0.24
P ₂ O ₅					0.29	0.31
S %						(d)
sum						
Sc ppm	15.7	15.8	12		(b)	
V						
Cr	1710	1710	1437		(b)	
Co	36	24.9	30		(b)	
Ni	167	137	600	195	(c)	
Cu						
Zn	1.9	1.9	2.3	2.9	(c)	
Ga						
Ge ppb	135	216	320	320	(c)	
As						
Se	57	110	59	73	(c)	
Rb	3	3.2	2.8		(c)	
Sr						
Y						
Zr						
Nb						
Mo						
Ru						
Rh						
Pd ppb			31.5	11.6	(c)	
Ag ppb	0.7	0.7	5.9	0.98	(c)	
Cd ppb	5.4	7.4	5.4	5	(c)	
In ppb						
Sn ppb						
Sb ppb	1.7		33	1.51	(c)	
Te ppb	7.2		8.7		(c)	
Cs ppm	0.11	0.141	0.109		(c)	
Ba						
La	27.7	27.5	23.4		(b)	
Ce	74	73	65		(b)	
Pr						
Nd						
Sm	12.2	12.4	10.2		(b)	
Eu	1.41	1.41	1.44		(b)	
Gd						
Tb	2.9	2.7	2.6		(b)	
Dy						
Ho						
Er						
Tm						
Yb	9.4	9.3	7.9		(b)	
Lu	1.27	1.27	1.09		(b)	
Hf	10.7	9.9	8.3		(b)	
Ta	1.2	1.4	1.4		(b)	
W ppb						
Re ppb	0.34	0.32	2.6	0.56	(c)	
Os ppb	3.6	3.1	34	6.3	(c)	
Ir ppb	3.2	3.5	27	5.4	(c)	
Pt ppb						
Au ppb	2	2	5.6	3.4	(c)	
Th ppm	4.6	4.4	3.9		(b)	
U ppm	1.1	1.13	1.04	1.38	(c)	

technique: (a) AAS, (b) INAA, (c) RNAA, (d) elec. Probe

**FIRST
SLAB**

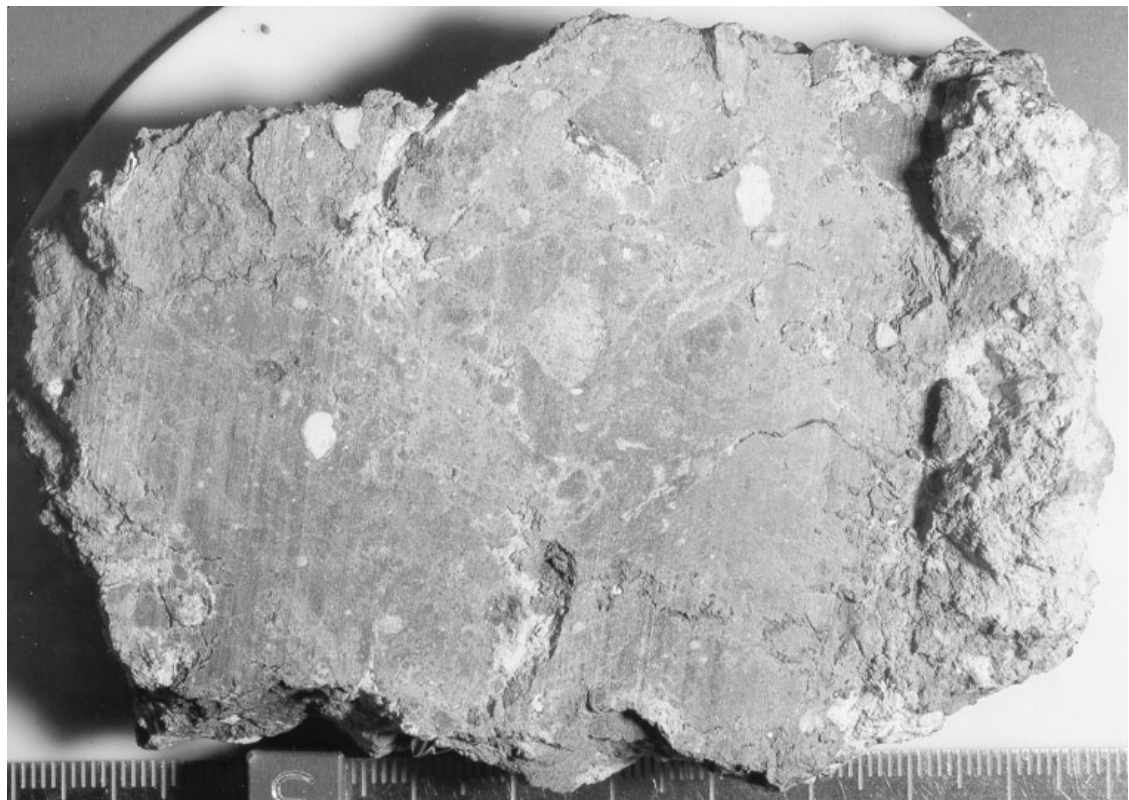


Figure 23: Photo of first slab of 73215 showing clasts studied by James Consortium (side facing second slab, figure 9). NASA S73-38458. Cube is 1 cm.

BC —————
GS ————— **FIRST
SLAB**

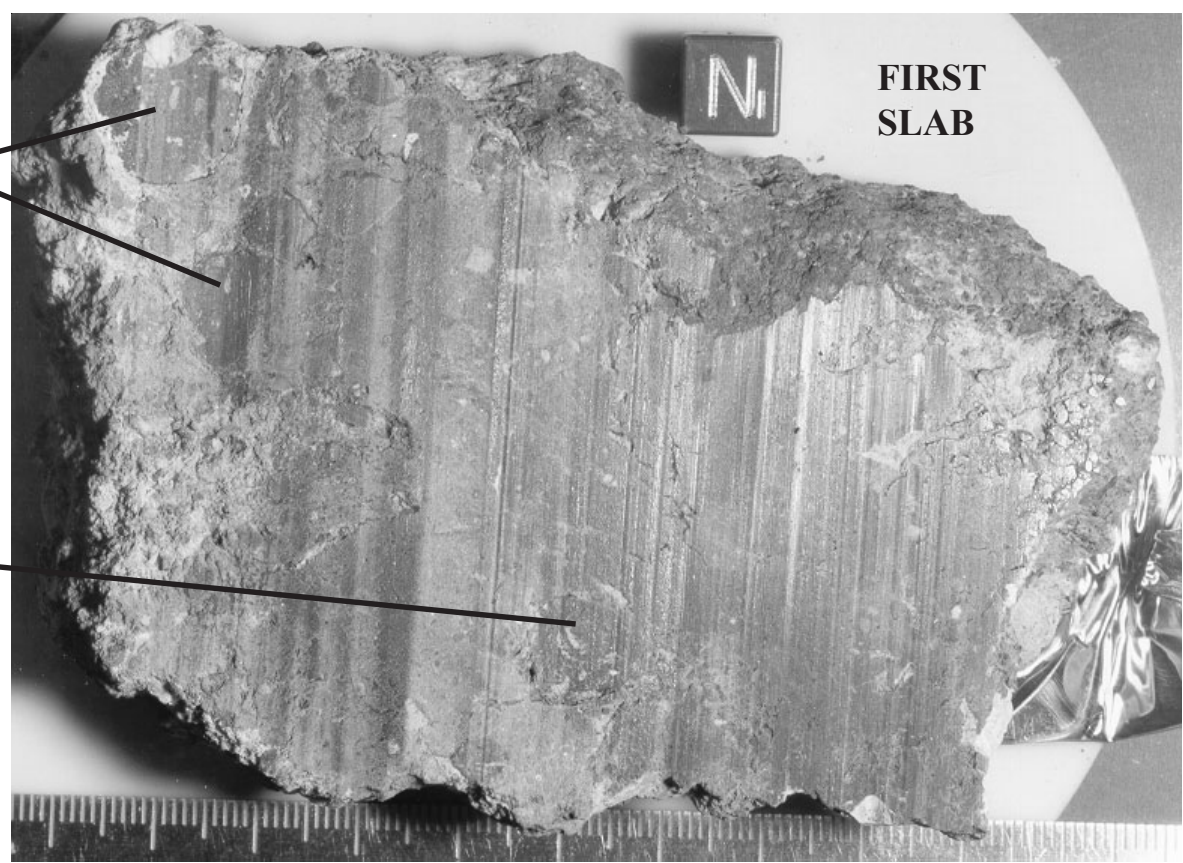


Figure 24: Photo of reverse side of first slab of 73215 (side facing ,8). NASA S73-38451. Cube is 1 cm.

FIRST
SLAB

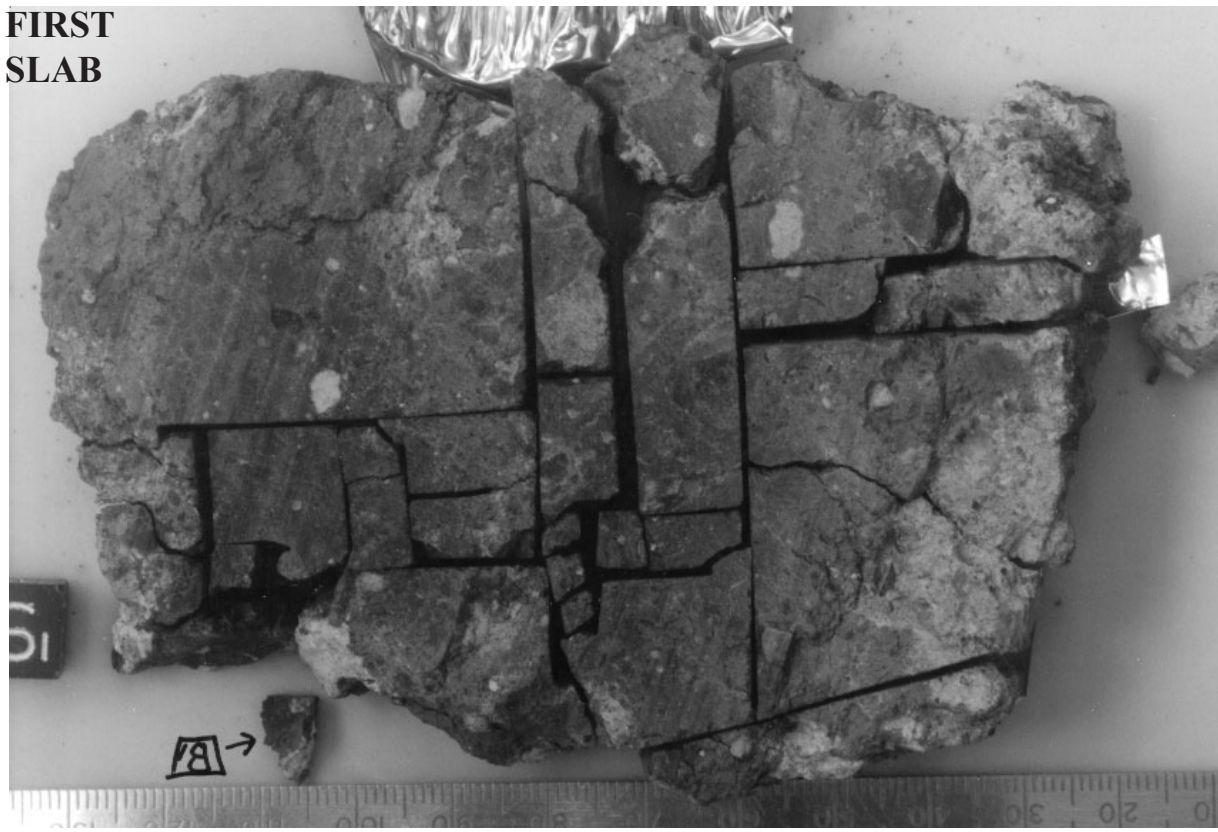


Figure 25a: Exploded parts diagram for first slab cut from 73215. NASA S74-17775. Cube is 1 cm.

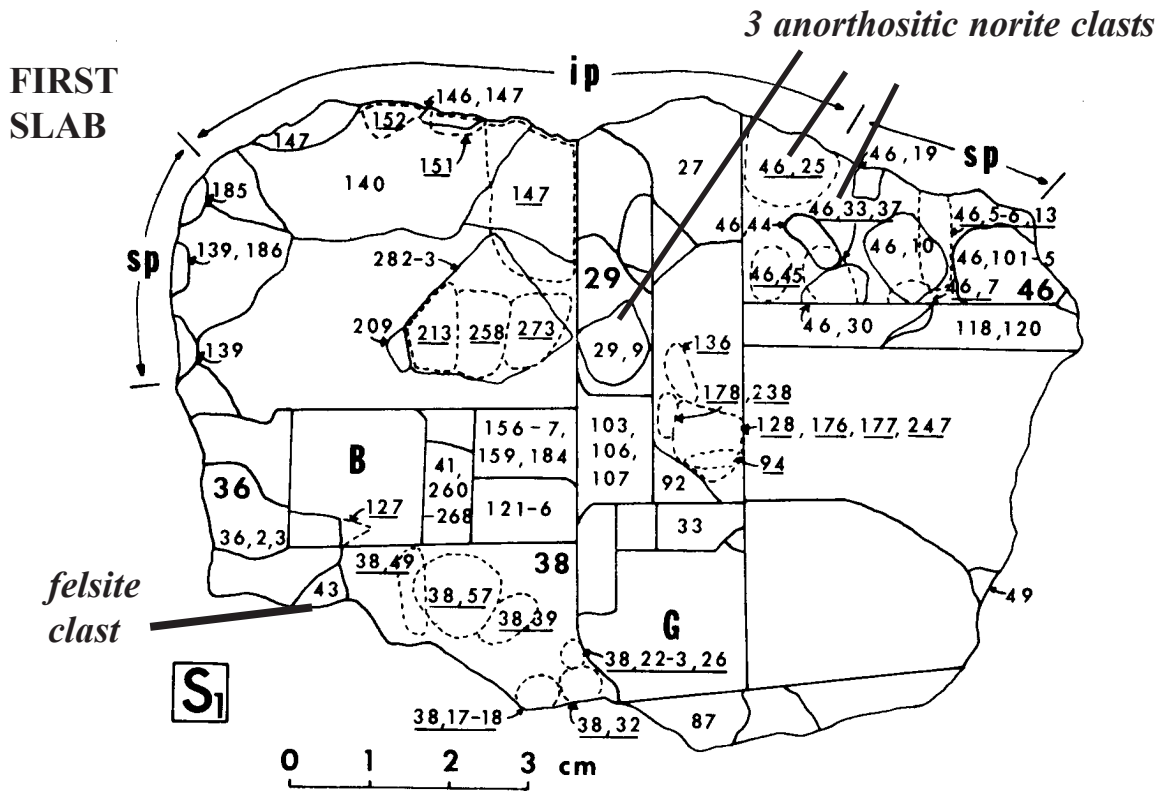


Figure 25b: Diagram used by James and Blanchard (1976) to show location of subsamples allocated to James Consortium members. "ip" stands for intensely pitted surface.

C Meyer
2006

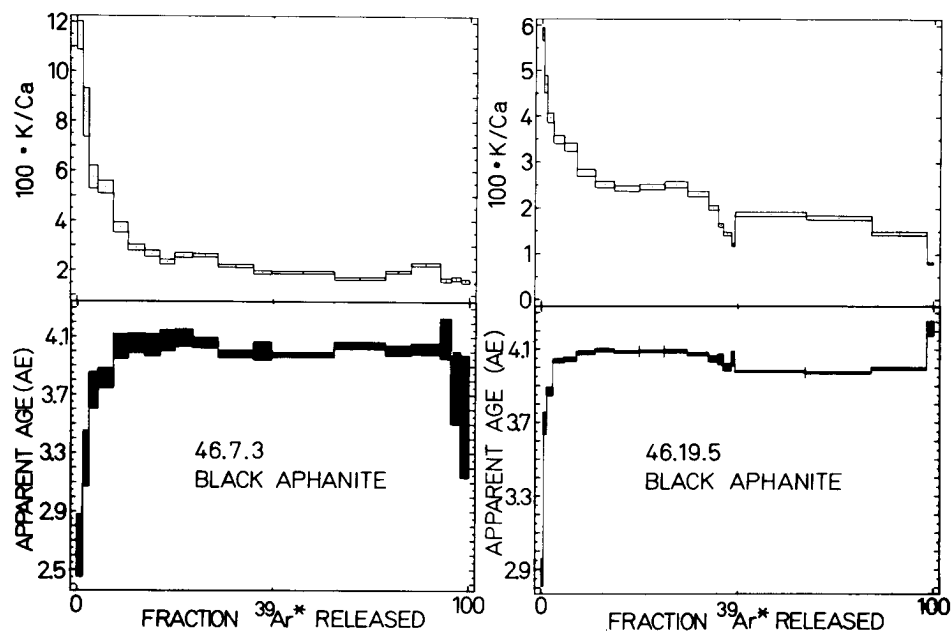
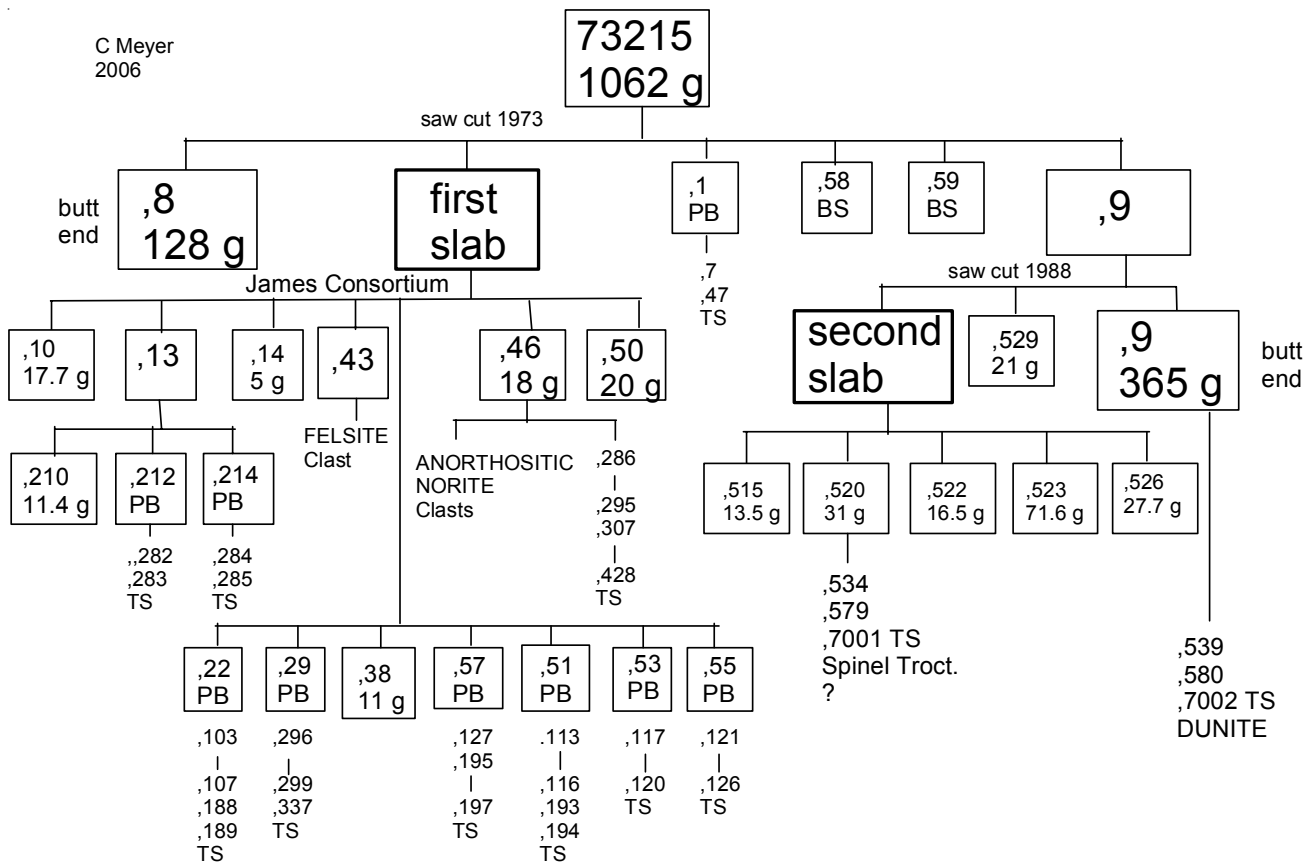


Figure 26: Examples of argon-argon plateau ages obtained by Jessberger et al. 1977, 1978.